Eur. Phys. J. D **54**, 391–398 (2009)
DOI: 10.1140/epjd/e2009-00144-3

THE EUROPEAN PHYSICAL JOURNAL D

Regular Article

Non-Maxwellian electron energy distribution function in He, He/Ar, He/Xe/H_2 and He/Xe/D_2 low temperature afterglow plasma

R. Plasil[1,a], I. Korolov[1,2], T. Kotrik[1], P. Dohnal[1], G. Bano[2], Z. Donko[2], and J. Glosik[1]

[1] Department of Surface and Plasma Science, Faculty of Mathematics and Physics, Charles University in Prague, Czech Republic
[2] Research Institute for Solid State Physics and Optics of the Hungarian Academy of Sciences, Hungary

Received 12 September 2008 / Received in final form 7 January 2009
Published online 8 May 2009 –

Abstract. Experimental studies of the electron energy distribution function "EEDF" under well defined conditions in flowing afterglow plasma, using a Langmuir probe are reported. The EEDF is measured in He_2^+ and Ar^+ dominated plasmas and in XeH^+ and XeD^+ dominated recombining plasmas. He is used as a buffer gas at medium pressures in all experiments (1600 Pa, 250 K). The deviation of the measured EEDF from Maxwellian distribution is shown to depend on plasma composition and on the processes governing the plasma decay. The influence of energetic electrons produced during the plasma decay on the body and tail of the EEDF is observed. The mechanism of energy balance in afterglow plasma is discussed.

PACS. 52.20.Fs Electron collisions – 52.20.-j Elementary processes in plasmas – 52.70.Ds Electric and magnetic measurements

1 Introduction

Internally excited and especially metastable particles play an essential role in pulsed and decaying plasmas. The density of these particles can exceed the density of charged particles by several orders of magnitude. In low temperature plasma the overall energy stored in these excited neutral particles can be substantially higher than in ions and the potential energy of electrons. This excitation energy can be transferred to kinetic energy of electrons in inelastic collisions. Depending on the intensity of this process and the dissipation of the energy gained, the electron energy distribution function "EEDF" can change, and eventually the temperature of electrons can increase. The influence of inelastic processes on electron energy distribution functions in low temperature plasma has been studied theoretically and experimentally many times. Production of fast electrons in Penning ionisation and non-Maxwellian EEDFs were observed in many experiments [1–4]. Bi-Maxwellian EEDF and depletion of fast electrons due to inelastic collisions have also been frequently observed. In the majority of these experiments EEDFs were measured in non-isothermal plasmas with an electron temperature $T_e > 1$ eV, measurements in thermal plasma with $T_e \sim 300$ K are very exceptional [5]. In thermal plasma the EEDF at 300 K spans just over a few tenths of an eV, and the production of electrons with energy ∼1 eV is not overlapped by the EEDF body. This can significantly modify the tail of the EEDF. This is the case of helium flowing afterglow plasma, which contains He metastables He(2^3S) and He(2^1S) with excitation energies 19.8 eV and 20.6 eV, respectively [6,7]. If reactant gas with an ionisation energy lower than the excitation energy of the helium metastables is added to such a plasma, Penning ionisation takes place and fast electrons are produced. If Ar, Kr or Xe are used as reactant gases the plasma is dominated by atomic ions which recombine only very slowly [8]. In such plasmas the electron temperature, EEDF and its evolution can be studied very precisely. Here, we report measurements of the EEDF and its relaxation in near-thermal plasmas in flowing afterglow. Because the plasma temperature is very low, the production of electrons in sub 1 eV region and the depletion of the tail of the EEDF due to losses to the wall are observed to depend on the conditions in the plasma.

2 Experiment

A schematic of the flowing afterglow with Langmuir probe (FALP) used in the presented experiments is shown in Figure 1. Helium buffer gas flows through the glass discharge tube (12 mm in diameter), where the plasma is formed in a cylindrical microwave resonator applying a power from 10 W to 25 W. The plasma is then driven by a flow of the buffer gas into the stainless steel flow tube with diameter 50 mm, where reactants can be introduced via injection ports (P1, P2).

[a] e-mail: Radek.Plasil@mff.cuni.cz

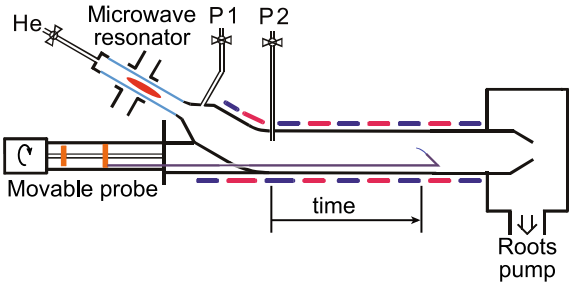

Fig. 1. (Color online) Schematic of FALP apparatus. Buffer gas flows from discharge region (upper left corner) towards the Roots pump (right). The plasma formed in the discharge is driven along the flow tube. The plasma parameters on the axis of the flow tube are measured by an axially movable Langmuir probe (from the port P2 up to the end of the flow tube).

The flow tube is kept at 250 K during the measurements. The parameters of the plasma in the axis of the flow tube are measured by an axially movable Langmuir probe over a range of ∼35 cm downstream from the second reactant inlet P2; this corresponds to a plasma decay time of up to 60 ms. The probe itself is made of a tungsten wire with a diameter of 18 μm and length 7 mm. Details of the FALP experiment are given in reference [7,9].

3 Measurement of plasma parameters

The basic principle of the plasma diagnostic using a Langmuir probe lays in the measurement of the voltage-current characteristics of the probe immersed into the plasma (I_{Pr} versus U_{Pr}). The electron density is determined from the slope of the linear section of the plot of I_{Pr}^2 versus U_{Pr}. The probe is calibrated for absolute electron density measurements using the well-established value of a recombination rate coefficient of O_2^+ ions [10–12]. From measured probe characteristic the electron density, the plasma potential and the floating potential can be obtained. The measured temporal evolutions of electron densities are plotted in Figure 2. Also plotted are differences between plasma and floating potential $\Delta = (U_{\mathrm{Pl}} - U_{\mathrm{fl}})$; this difference is proportional to electron temperature if the plasma has a Maxwell electron energy distribution function [12]. The actual electron temperature can be calculated from the probe characteristics under the assumption that the plasma has a Maxwellian (or close to Maxwellian) EEDF. The evolution of electron temperature along the flow tube, calculated from the measured probe characteristics are shown in Figure 2.

Interpretation of the observed evolutions along the flow tube in He_2^+ and Ar^+ dominated plasmas is relatively simple. The afterglow plasma in pure He after ∼35 ms of decay consists of very slowly recombining He_2^+ ions [10] and metastable $He(2^3S)$ [6,7]. The plasma predominantly decays by ambipolar diffusion, hence the exponential decay of electron density is observed. The decay of density of metastables is very slow and at the position of port P2 their density is higher than the ion density. This can be

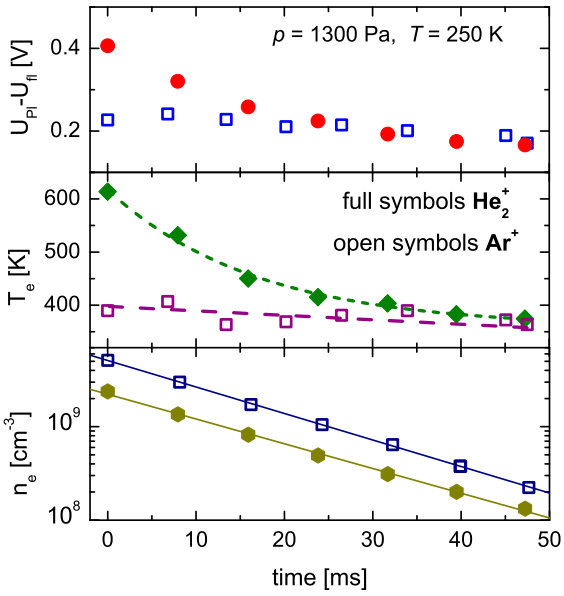

Fig. 2. (Color online) The evolution of afterglow plasma along the flow tube in He_2^+ (full symbols) and Ar^+ (open symbols) dominated plasmas. Upper panel: the difference between plasma and floating potential $\Delta = (U_{\mathrm{Pl}} - U_{\mathrm{fl}})$. Middle panel: the measured electron temperature evolutions in He_2^+ and Ar^+ dominated plasmas. Lower panel: the decays of electron densities along the flow tube.

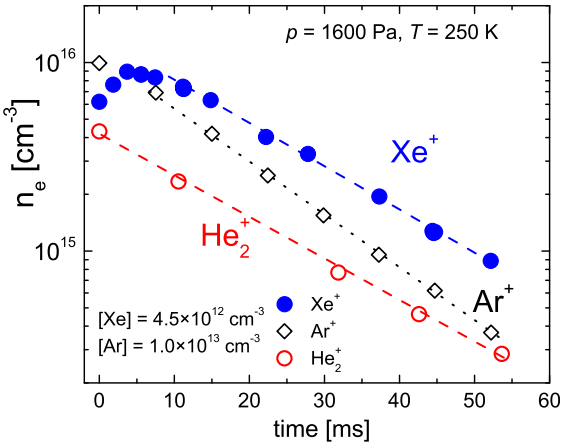

Fig. 3. (Color online) The measured decay of electron density in He_2^+ dominated plasma in pure He and the increase of the electron density in the afterglow plasma after injection of Xe via port P2. Indicated are the dominant ions. For comparison the electron density decay of argon plasma is plotted. In this case Ar is added to the afterglow via port P1.

demonstrated by adding a gas with ionisation energy lower than the excitation energy of metastables to the flow tube via port P2. Figure 3 presents the measured evolution of electron density after addition of Xe via port P2. Immediately after the addition of xenon, electrons and Xe^+ ions are produced in fast Penning ionisation.

In afterglow in pure helium, the metastables interact with electrons in superelastic collisions and as a consequence the electron temperature is higher than buffer gas

temperature (see Fig. 2). If metastables are removed by Penning ionisation, the plasma loses the source of heating and the electron temperature is close to 300 K. The question is how the heating of electrons is reflected in the EEDF. Instead of Xe, Ar or Kr can be used to remove metastables from a helium afterglow. In the majority of recombination studies a small admixture of Ar in He is used to remove metastables (see Fig. 3).

4 Measurement of EEDF in He_2^+ dominated decaying plasma

In some studies of plasmas a rough estimation of electron temperature is not sufficient and it is necessary to measure actual EEDF. These measurements are important if processes with strong dependence on electron energy are studied in afterglow plasma. Such studies are, for example, measurements of recombination rate coefficients. The measurement of EEDF along the flow tube also characterises the degree of relaxation of the afterglow plasma. Eventually it indicates the correct use of electron temperature for the characterisation of electron gas. The example of measured probe characteristics and corresponding second derivative I''_{Pr} are shown in Figure 4. The probe characteristics were measured at port position P2; this corresponds to the plasma decay time $\tau = 35$ ms.

At positive probe potentials with respect to the plasma potential, for $U_{\mathrm{Pr}} > U_{\mathrm{Pl}}$, there is a section of "saturated electron current". At $U_{\mathrm{Pr}} < U_{\mathrm{fl}}$ there is "saturated ion current". The region in between is called the "transition region". The probe characteristics were fitted in the region of the saturated ion current [12] and the fit was extrapolated towards the plasma potential to obtain I_{i} in the transition region (see Fig. 4), where it cannot be measured. By subtraction of the ion current from the overall probe current the corresponding electron current to the probe is obtained: $I_{\mathrm{e}} = I_{\mathrm{Pr}} - I_{\mathrm{i}}$.

The EEDF ($f(\varepsilon)$) can be calculated from the second derivative of the electron current to the probe using Druyvesteyn formula (the values obtained using this formula are indicated as $f_{\mathrm{D}}(\varepsilon)$) [7,12]. For $(U_{\mathrm{Pr}} - U_{\mathrm{Pl}}) < 0$

$$f_{\mathrm{D}}(\varepsilon) = f_{\mathrm{D}}(q(U_{\mathrm{Pr}} - U_{\mathrm{Pl}})) = \frac{2\sqrt{2m_{\mathrm{e}}}}{n_{\mathrm{e}} q^2 A} \sqrt{\frac{U_{\mathrm{Pr}} - U_{\mathrm{Pl}}}{q}} \frac{d^2 I_{\mathrm{e}}}{dU_{\mathrm{Pr}}^2}, \quad (1)$$

where U_{Pr} is the probe potential and $f_{\mathrm{D}}(\varepsilon)$ is the EEDF at energy $\varepsilon = q(U_{\mathrm{Pr}} - U_{\mathrm{Pl}})$ normalised to 1. The electron charge $q < 0$. Note that in the formula the electron part of the probe current I_{e} is used to obtain the EEDF. Due to the large difference in electron and ion masses and because of the nature of the dependence of ion current on the probe potential $I_{\mathrm{i}}(U_{\mathrm{Pr}})$ we can, to a rather good approximation, use $I''_{\mathrm{Pr}} = I''_{\mathrm{e}} + I''_{\mathrm{i}} \approx I''_{\mathrm{e}}$. In Figure 4 both I''_{Pr} and I''_{e} are plotted, the difference is negligible. It is obvious that at our experimental conditions (pressures 660–2000 Pa) the correction of EEDF accounting for ion current can be neglected. The plasma U_{Pl} and the floating U_{fl} potentials are

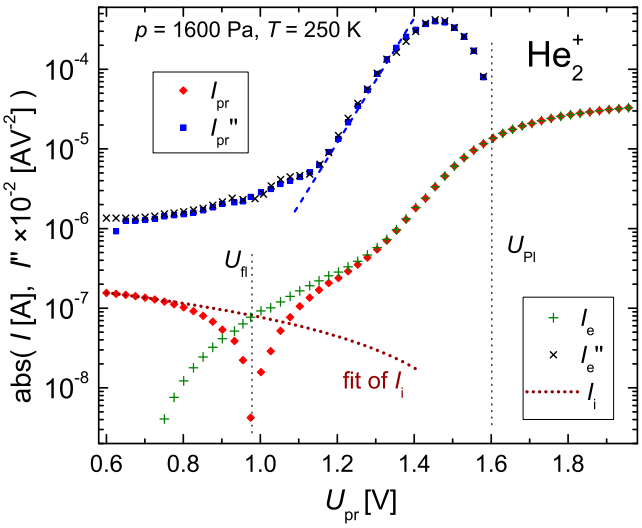

Fig. 4. (Color online) The probe characteristic I_{Pr} versus U_{Pr} and its second derivative I''_{Pr} measured in He afterglow 35 ms after the discharge. Indicated is the plasma potential U_{Pl}, the floating potential U_{fl} and the fit of the ion current I_{i}. From the extrapolation of the ion current I_{i} and from the probe current the electron current to the probe I_{e} and its second derivative I''_{e} were calculated.

given by the conditions $I''_{\mathrm{Pr}} = 0$ and $I_{\mathrm{Pr}} = 0$, respectively. More detailed description of Langmuir theory is given in reference [12].

As follows from the Druyvesteyn formula the second derivative I''_{Pr} is proportional to $f_{\mathrm{D}}(\varepsilon)/\sqrt{\varepsilon}$. If the EEDF is Maxwellian then a semi-logarithmic plot of I''_{Pr} versus ε gives a straight line. The fitted straight line to the data plotted in Figure 4 corresponds to Maxwellian EEDF with $k_{\mathrm{B}}T_{\mathrm{e}} \sim 0.05$ eV. It is evident that for $\varepsilon = q(U_{\mathrm{Pr}} - U_{\mathrm{Pl}}) > 0.5$ eV the measured EEDF has an excess of electrons in comparison with Maxwellian EEDF. We assume that the observed high-energy electrons in He afterglow originate from reactions of two metastables, $\mathrm{He^m} + \mathrm{He^m} \rightarrow \mathrm{He_2^+} + \mathrm{e^-}(\varepsilon)$, where $\varepsilon \sim 15$ eV. Part of these fast electrons can escape the plasma because the ambipolar field is not strong enough to control their flow. Some of these fast electrons lose their energy in elastic collisions with He atoms and are cooled down to a lower energy. We can see these electrons on measured curves as an excess above the Maxwellian EEDF (enhancement of the tail of the EEDF, see Fig. 4). If electrons have an energy below 0.5 eV, the electron-electron energy exchange is very effective, the maxwellisation is fast and the EEDF is very close to Maxwellian. Due to the integral effect we can see that the electron temperature is significantly higher than the buffer gas temperature during the early afterglow (see Fig. 2). Beyond this point the temperature slowly decreases along the flow tube with decreasing metastable density.

The Druyvesteyn formula should be used with care at higher pressures because the electron current to the probe is influenced by electron-atom collisions close to the probe. We studied the necessary correction of the EEDF,

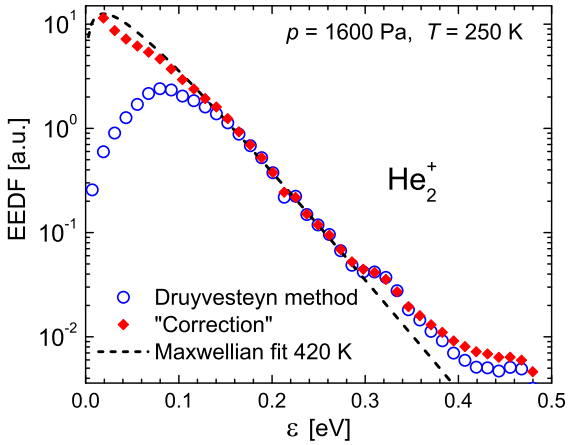

Fig. 5. (Color online) The electron energy distribution function "EEDF" measured in the very late afterglow in the helium buffered plasma dominated by ions He_2^+. In first approximation the EEDF is obtained from the probe characteristic using Druyvesteyn method (open symbols). Better approximation is obtained with correction to influence of collisions in vicinity of the probe (closed symbols) [7]. The dashed curve indicates Maxwellian EEDF fitted to measured data for $\varepsilon > 3k_BT_e$.

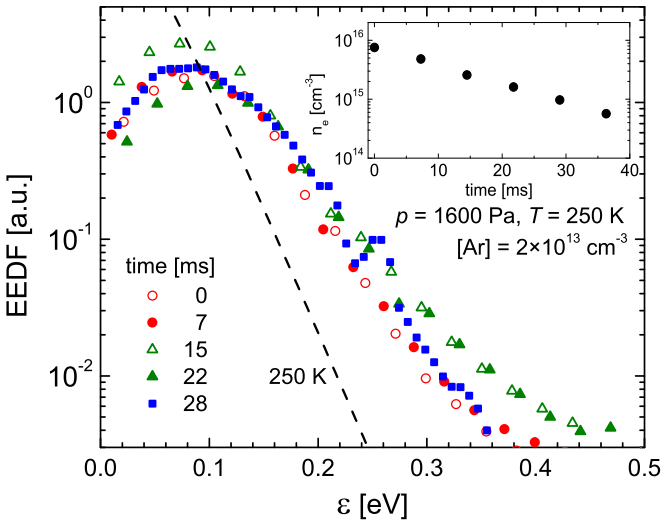

Fig. 6. (Color online) The evolution of electron energy distribution function along the flow tube in Ar^+ dominated plasma in He with admixture of Ar. The plotted EEDFs are normalised to 1. In the inset the corresponding electron density n_e decay is plotted.

see reference [7] and references therein. The EEDF obtained from Druyvesteyn formula and the EEDF after the correction are plotted in Figure 5. Note that the correction is significant only for energies $\varepsilon < 3k_BT_e$. Because in the present study we concentrate on the EEDF at higher energies ($\varepsilon > 3k_BT_e$) we will not pay attention to invalidity of Druyvesteyn formula in low energy region.

The EEDF plotted in Figure 5 was measured 35 ms after the discharge, nevertheless we can see that at energies >0.3 eV there is small excess of fast electrons. The helium metastables heat the electrons even in late afterglow (see above discussion in connection with data plotted in Fig. 4 and discussion in Ref. [7]). The measurements show the very high accuracy and sensitivity of our apparatus.

If Ar is added to the $He_2^+/He^m/e^-$ plasma, the metastables are removed by Penning ionisation and Ar^+/e^- plasma is formed. The evolution of EEDF measured in such a plasma is shown in Figure 6. The EEDFs are nearly Maxwellian over the whole range of electron energies covered. The electron temperature obtained is $T_e \sim 340$ K i.e. it is slightly higher than T_{He}, $\Delta T_e \sim +90$ K. The increase can be caused by the presence of excited Ar^+ ions in the $^2P_{1/2}$ spin state, with excitation energy $\Delta\varepsilon = 0.18$ eV [13]. These excited ions formed in the Penning ionisation can transfer energy to electrons by superelastic collisions. This phenomenon was observed in Kr^+ and Xe^+ dominated plasmas. From the present study and also from other experiments [7] we can see that our measurements suffer from the "apparatus effect", which increases the apparent electron temperature. The measured temperature was $\delta \sim +70$ K higher with respect to the buffer gas temperature. This systematic increase is probably due to fluctuations of the plasma potential, probe potential and inhomogeneity of the probe surface. If the potential on the probe against plasma potential fluctuates, it will increase the apparent temperature measured from the probe characteristics.

Note that EEDFs do not change significantly along the flow tube and if we consider the above mentioned "apparatus effect" $\delta \sim +70$ K we can conclude that the Ar^+/e^- plasma is cold and thermal with electron temperature close to the buffer gas temperature. We observe a small excess of fast electrons but this is already within the noise limit and it corresponds to less than 0.01% of electrons. More pronounced effects were observed in recombining plasmas as will be demonstrated further in the text. This cold relaxed Ar^+/e^- plasma is used in our FALP experiments to form plasmas dominated by desired ions. In the present study this will be XeH^+/e^- and XeD^+/e^- plasmas.

5 Measurements of EEDF in recombination governed low temperature plasma in He/Ar/Xe/H_2 and He/Ar/Xe/D_2

The different situation is in the afterglow plasma where excited particles (ions and/or neutrals) are produced in ion molecule reactions or in dissociative recombination. We will discuss measurements of the EEDF in afterglow plasma under the conditions that were used for measurements of recombination rate coefficients of XeH^+ and XeD^+ ions. In these experiments, helium is used as a buffer gas. The discharge glows in pure He and Ar is added immediately downstream from the discharge region via the first reactant port P1 to form the Ar^+/e^- plasma. The H_2/Xe (or D_2/Xe) mixture is introduced into the flow tube via the second reactant port P2 and the XeH^+/e^- (or XeD^+/e^-) dominated plasma is formed. The flow rates of

Table 1. The main reactions taking place in the formation of XeH^+ and XeD^+ ions in He/Ar/Xe/H_2 and He/Ar/Xe/D_2 plasmas, respectively.

No.	Reaction	Rate coefficient ($cm^3\,s^{-1}$)	Reference
1	$Ar^+ + Xe \rightarrow Xe^+ + Ar$	4×10^{-13}	[14]
	XeH^+ formation		
2a	$ArH^+ + Xe \rightarrow XeH^+ + Ar$	5×10^{-10}	*
3a	$H_3^+ + Xe \rightarrow XeH^+ + H_2$	2.4×10^{-9}	[15]
4a	$XeH^+ + e^- \rightarrow$ products	8×10^{-8}	***
	XeD^+ formation		
2b	$ArD^+ + Xe \rightarrow XeD^+ + Ar$	5×10^{-10}	*
3b	$D_3^+ + Xe \rightarrow XeD^+ + D_2$	1.7×10^{-9}	**
4b	$XeD^+ + e^- \rightarrow$ products	8×10^{-8}	***

* Estimation based on Langevin rate coefficient.
** Estimation using data for reaction of H_3^+ with Xe [15].
*** Present experiment, the values measured at 1600 Pa and 250 K.

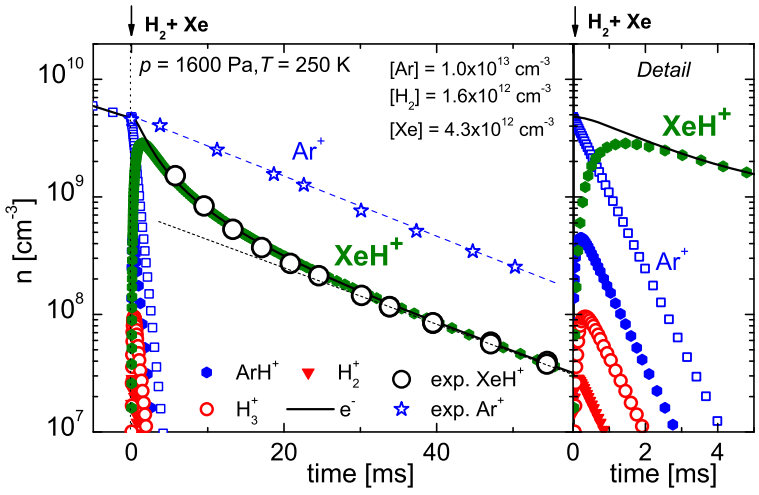

Fig. 7. (Color online) The calculated plasma formation and decay along the flow tube in He/Ar/Xe/H_2 mixture. We do not plot whole evolution between discharge and port P2, plotted is only the section shortly before port P2. Data were obtained by solving the set of partial differential equations corresponding to considered processes. The diffusion and the recombination losses are also included in the model. Plotted is also the electron density decay measured at corresponding conditions (large circles). For comparison the decay measured in He/Ar mixture dominated by Ar^+ ion is also plotted; this decay is governed by diffusion losses only.

the reactant gases H_2 (or D_2) and Xe are controlled and regulated independently on each other. The key reactions taking place in the formation of XeH^+ (XeD^+) ions are listed in Table 1.

The reactions leading to formation of an Ar^+ dominated plasma and the reactions leading to the formation of H_3^+ and D_3^+ ions are not included in the Table 1, since they are described and discussed in our previous publications (see e.g. [16,17]). Since the proton affinity of Xe is larger than the proton affinity of hydrogen (the difference is ~0.75 eV), XeH^+ ions do not react with H_2. Hence, XeH^+ ions are removed from the afterglow plasma only by the diffusion and by dissociative recombination. The actual experimental conditions were optimised by a numerical model. The calculated evolution of ionic composition during the afterglow in He/Ar/Xe/H_2 plasma is shown in Figure 7. The zero of the time scale corresponds to position of port P2 (injection of H_2 and Xe). The fast transition from Ar^+ dominated plasma to XeH^+ dominated plasma immediately after injection of reactant gases is shown in the detail (right panel). Even if the mixing of the gases (the end correction) is taken into account the XeH^+ dominated plasma will be formed within 3 ms. The sequence of the key reactions can be written as:

$$Ar^+ + H_2 \rightarrow (ArH^+ \text{ or } H_2^+) + (Xe, H_2) \rightarrow (XeH^+ \text{ or } H_3^+) + (Xe, H_2) \rightarrow XeH^+. \quad (2)$$

All these processes were considered in the kinetic model. The previously discussed EEDFs measured in the Ar^+ dominated plasma show that the plasma is relaxed and cold before injection of Xe and H_2. In the sequence of the reactions starting from Ar^+ and terminating with XeH^+ internally excited ions can be formed. The excess of energy in XeH^+ can be up to ~2.8 eV if the exothermicity of all the reactions is transferred to an internal excitation of XeH^+, which is not very probable. What is more probable is that the exothermicity of the last proton transfer, leading to XeH^+ formation, will be partially used for internal excitation of XeH^+. If a XeH^+ ion is formed from H_3^+, the resulting exothermicity is 0.75 eV; if it is formed from ArH^+, the exothermicity is 1.3 eV. Nevertheless, if a

XeH^+ ion has an internal excitation higher than 0.75 eV, it can transfer a proton to H_2 and form H_3^+, which will in a consequent reaction with Xe form a new XeH^+. In this sequence of reactions part of internal energy will be dissipated. The consequence of this loop is that internal excitation energy of XeH^+ will be lower than 0.75 eV. The recombination of XeH^+ ions is relatively slow and for our experimental conditions ions on average survive 10–20 ms before recombination, see Figure 7 (for details of recombination see Refs. [8,18]). During this time XeH^+ ions have millions of collisions with He atoms and several collisions with H_2 or Xe. In these collisions an internal excitation can be quenched or partly quenched, but not necessarily. For example, the quenching of vibrational excitation of N_2^+ ($v = 1$) is, in collisions with He or N_2, very ineffective [19]. The quenching was studied many times; see the review on quenching in helium buffer gas by Ferguson [20].

In superelastic collisions of internally excited ions with electrons the internal excitation can be transferred to kinetic energy of electrons. We already mentioned our observation of such energy transfer in He_2^+ dominated afterglow in pure He, see Figures 4 and 5 and the above discussion (for more details see Ref. [7]).

In order to define conditions in the flowing afterglow plasma used for the study of recombination of H_3^+, HCO^+, KrH^+, XeH^+ and XeD^+ ions [5,18,21] we measured EEDF in different mixtures of reactant gases used for the preparation of plasmas dominated by these ions. Because of the expected dependencies of recombination rate coefficients of these ions on electron energy we measured EEDF along the flow tube i.e. upstream in the formation region and downstream in the recombination and diffusion dominated region. Further we will concentrate on XeH^+ and XeD^+ dominated plasmas. In Figure 8 the EEDFs measured in XeH^+ study are plotted. The reactant densities used in this particular experiment are slightly higher than the densities used in the calculation (see Fig. 7) which is why the formation is slightly faster. We fitted the measured EEDFs with a Maxwellian distribution (see plotted lines in Fig. 8) and we obtained the corresponding electron temperatures. If we consider the above discussed correction in low energy region $<3k_BT_e$, we can see from the plotted data that the EEDFs are in very good approximation with a Maxwellian. Nevertheless, we have observed in the EEDFs a group of "high-energy electrons" with energies 0.4–0.8 eV. This group contains only a few percent of all electrons ($n_e^{fast}/n_e \ll 1$). Note that in this energy region the measured EEDF is far higher than the noise level, which is $\ll 0.1\%$ (see above discussion of EEDF measured in Ar^+ dominated plasma). We expect that in this context these "high-energy electrons" are formed in superelastic collisions of "cold electrons" from the Maxwellian part of EEDF with internally excited particles. The question is, what sort of heavy particle is responsible for this process? As can be seen from the ion density evolutions plotted in Figure 7, we can rule out all ions that are present along the entire flow tube, with exception of XeH^+. From this estimation we can expect that the internal excitation of these ions is lower than 0.75 eV.

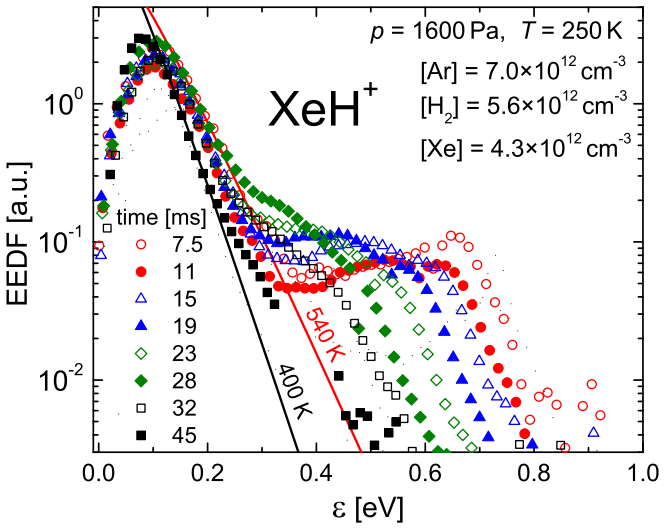

Fig. 8. (Color online) Evolution of EEDF in He/Ar/Xe/H_2 plasma obtained from measured characteristics of Langmuir probe. In low energy region (<0.15 eV), the EEDFs are expected to be Maxwellian [7]. The solid curves correspond to Maxwellian electron energy distributions fitted to the measured data for the decay time 7.5 ms and 45 ms. The plotted EEDFs are normalised to 1. Experimental conditions are indicated.

The origin of the electron energy from the internal excitation of XeH^+ can be supported by the observation that the fraction of "high-energy electrons" in the EEDF is constant (ratio n_e^{fast}/n_e). As can be seen from the plots (Fig. 8) of the normalized measured EEDFs, the relative density of the fast electrons decreases by approximately a factor of two during first 28 ms. During this time the electron density decays by a factor of twenty (Fig. 7). The nearly constant value of the ratio indicates that the production and losses of the "high-energy electrons" are in equilibrium or close to equilibrium. If the "high-energy electrons" are formed in collisions of exited XeH^+ ions with the "cold electrons", then the formation rate is proportional to $[XeH^{+*}]n_e$, where $[XeH^{+*}]$ is number density of excited ions. In quasi neutral plasma we can write $[XeH^{+*}]n_e = \xi[XeH^+]n_e = \xi n_e n_e$; where ξ is the fraction of ions in the excited state. At energies under 1 eV the "high-energy electrons" are thermalised by collisions with the "cold electrons" so the rate of losses is proportional to $n_e^{fast}n_e$. From this follows that during the decay the ratio $n_e^{fast}/n_e \sim \xi$. The observed slow changes of n_e^{fast}/n_e can indicate slow decay of relative density of XeH^{+*}.

We cannot exclude superelastic collisions of electrons with excited neutral products of recombination of XeH^+ ions. If these excited states are long lived, their density will only slowly decay along the flow tube and fast electrons will be produced along the whole flow tube, as we observed in the experiment. These excited particles can have considerably higher excitation energy than just 0.75 eV and they can produce electrons with higher energy.

We also studied EEDF in He/Ar/Xe/D_2 plasma dominated by XeD^+ ions. The kinetics of the formation of

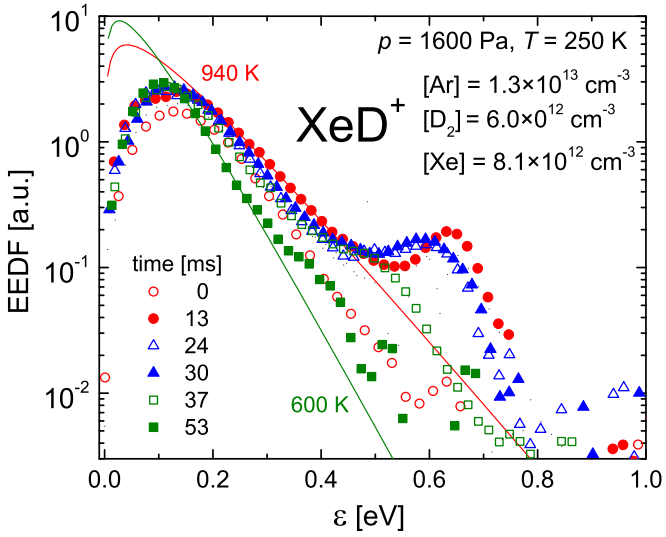

Fig. 9. (Color online) The measured evolution of EEDF in He/Ar/Xe/D_2 plasma. The solid curves correspond to Maxwellian electron energy distribution fitted to the measured data for the decay times 13 ms and 53 ms. The plotted EEDFs are normalised to 1. Experimental conditions are indicated.

XeD^+ is similar to the formation of XeH^+. Both ions have the same recombination rate coefficient [18], so one can expect very similar behaviour of the EEDF in the decaying plasma under identical conditions. Surprisingly, we observed some very pronounced differences, shown in Figure 9. The main difference is in the temperature of the decaying plasma: at decay time 13–15 ms the temperatures are ∼500 K and ∼940 K for XeH^+ and XeD^+ dominated plasma, respectively. At the end of the flow tube the temperature is higher (600 K) in XeD^+ dominated plasma. The maximum energy of the "high-energy electrons" group is 0.65 eV, similar to the XeH^+ in this study. We can only speculate that the isotope effect is connected with differences in energy levels of both ions.

6 Discussion and conclusions

If the density of the excited particles (the ions or the neutral products of recombination processes) is comparable with the electron density at the position of the port P2 ($\sim 10^{10}$ cm^{-3}) and it decays along the flow tube then we can consider it as a source of "high-energy electrons". The source can have an intensity $J = 10^{12}$–10^{14} cm^{-3} s^{-1} depending on experimental conditions. In large plasma in helium buffer gas, where the influence of the wall is negligible, fast electrons are cooled by electron-electron "Coulomb" (e-e) and electron-helium atom (e-He) collisions. We have estimated the role of these processes in numerical calculations assuming different intensities of source "high-energy electrons". The numerical simulation describes the temporal evolution of the EEDF in the presence of e-e and e-He collisions. The Monte Carlo approach was used for electron-neutral collision modelling. electron-electron Coulomb collisions were treated by Nanbu's theory of cumulative small angle scattering [24]. The calculations give bi-Maxwellian EEDF. The temperature of the EEDF body in He_2^+ dominated plasma depends on the intensity of the source. In He_2^+ dominated plasma we obtained a qualitative agreement of experimental and calculated EEDFs. The measured population of the EEDF tail is higher than the one obtained from the calculations. The difference between the calculated and measured data in He_2^+ dominated afterglow indicates that in the afterglow plasma the transfer of energy from fast electrons to slow electrons is more effective than was considered in the calculations. In our plasma the electron energy relaxation length λ_E is comparable to the characteristic dimensions of the flow tube, $\lambda_D \sim r/2.4 \sim 1$ cm, where r is the flow tube radius (see discussions in references [23,25]). It is considered that plasma is local if value $p\lambda_D > 1.3$ kPa cm and nonlocal if $p\lambda_D < 1.3$ kPa cm [22]. With value $p\lambda_D \sim 1.3$ kPa cm we are just in the transition region, where the EEDF will be dependent also on the electron density. We assume that the mentioned effective energy transfer is given by the electric field of ambipolar diffusion. Some of the fast electrons will overcome the ambipolar field and flows to the tube wall. As a consequence the ambipolar field increases. This field then traps and heats slow electrons. In actual conditions of flowing afterglow plasma the heating of electrons via this mechanism is more intensive than the heating (energy transfer from high energy electrons) from e-e and e-He collisions. By the inclusion of an electric field in our calculations we improved the agreement with the experimental data but we still only have a qualitative agreement.

The situation is even more complicated in the interpretation of data obtained in XeH^+ and XeD^+ dominated plasmas. In the early afterglow the superelastic collisions of "cold electrons" with excited ions (with excitation energy <0.75 eV) are probably the main source of hot electrons. This is reflected in the measured EEDF, which have high-energy groups of electrons with energy under ∼0.75 eV. In later afterglow the fast energy group diminishes and we observe a cut of the high-energy part of the measured EEDF, this can be connected with transition to a nonlocal character of the plasma and with an increasing in the excitation of ions (parameter ξ in above discussion).

We have measured EEDFs in different experimental conditions in nearly thermal afterglow plasmas; we have observed deviation of EEDFs from Maxwellian distribution. The deviation is very small in cold Ar^+ dominated afterglow, higher in He_2^+ dominated afterglow and very pronounced in XeH^+ and XeD^+ recombination dominated afterglow plasma. To our knowledge this is the first measurement of EEDFs in nearly thermal plasma (300–1000 K) indicating the role of superelastic collisions on electron heating, on plasma decay and the rate of the electron temperature relaxation. The effective recombination rate coefficient (α_{eff}) measured in an afterglow plasma (FALP experiments [26]) with Maxwellian EEDF (temperature T) and an additional small "group of fast electrons" ($n_e^{fast}/n_e \ll 1$) is in good approximation given by the

formula (see e.g. [18]): $\alpha_{\rm eff}(T) = \alpha_{\rm slow}(T) + \alpha_{\rm fast} n_{\rm e}^{\rm fast}/n_{\rm e}$. This has to be considered in data analysis. Also important is the higher electron temperature in comparison with the buffer gas temperature. In the present experimental conditions the small deviation of EEDF from Maxwell distribution ($n_{\rm e}^{\rm fast}/n_{\rm e} < 0.04$) is not playing a role in the determination of the recombination rate coefficient (see also Ref. [18])

This work is a part of the research plan MSM 0021620834 financed by the Ministry of Education of the Czech Republic and was partly supported by GACR (202/07/0495, 202/08/H057) by GAUK 53607, GAUK 124707 and GAUK 86908. This work was supported also by OTKA, grant No. 048389.

References

1. N.B. Kolokolov, A.A. Kudrjavtsev, A.B. Blagoev, Physica Scripta **50**, 371 (1994)
2. V.I. Demidov, C.A. DeJoseph Jr., Rev. Sci. Instrum. **77**, 116104 (2006)
3. V.M. Alexandrov, U. Flender, N.B. Kolokolov, O.V. Rykova, K. Wiesemann, Plasma Sources Sci. Technol. **5**, 523 (1996)
4. P. Spanel, L. Dittrichova, D. Smith, Int. J. Mass Spectrom. **129**, 193 (1993)
5. J. Glosik, R. Plasil, P. Zakouril, V. Poterya, J. Phys. B: At. Mol. Opt. Phys. **34**, 2781 (2001)
6. J. Glosik, O. Novotny, A. Pysanenko, P. Zakouril, R. Plasil, P. Kudrna, V. Poterya, Plasma Sources Sci. Technol. **12**, S117 (2003)
7. I. Korolov, R. Plasil, T. Kotrik, P. Dohnal, O. Novotny, J. Glosik, Contrib. Plasma Phys. **48**, 461 (2008)
8. I. Korolov, O. Novotny, R. Plasil, P. Hlavenka, T. Kotrik, M. Tichy, P. Kudrna, J. Glosik, A. Luca, Czech. J. Phys. Suppl. B **56**, 854 (2006)
9. M. Larsson, A.E. Orel, *Dissociative Recombination of Molecular Ions* (Cambridge University Press, Cambridge, 2008)
10. A.I. Florescu-Mitchell, J.B.A. Mitchell, Phys. Rep. **430**, 277 (2006)
11. J. Glosik, G. Bano, R. Plasil, A. Luca, P. Zakouril, Int. J. Mass Spectrom. **189**, 103 (1999)
12. J.D. Swift, M.J.R. Schwar, *Electrical Probes for Plasma Diagnostics* (Iliffe, London, 1970)
13. S.J. Buckman, P. Hammond, G.C. King, F.H. Read, J. Phys. B: At. Mol. Phys. **16**, 4219 (1983)
14. V.G. Anicich, *An Index of the Literature for Bimolecular Gas Phase Cation-Molecule Reaction Kinetics*, JPL publication 03-19 (Pasadena, California, 2003)
15. A. Le Padellec, S. Laube, O. Sidko, C. Rebrion-Rowe, B.R. Rowe, B. Sarpal, J.B.A. Mitchell, J. Phys. B: At. Mol. Opt. Phys. **30**, 963 (1997)
16. R. Plasil, J. Glosik, V. Poterya, P. Kudrna, J. Rusz, M. Tichy, A. Pysanenko, Int. J. Mass Spectrom. **218**, 105 (2002)
17. V. Poterya, J. Glosik, R. Plasil, M. Tichy, P. Kudrna, A. Pysanenko, Phys. Rev. Lett. **88**, 044802 (2002)
18. R. Plasil, I. Korolov, T. Kotrik, J. Glosik, Int. J. Mass Spectrom. **275**, 80 (2008)
19. M. Kriegel, R. Richter, W. Lindinger, L. Barbier, E.E. Ferguson, J. Chem. Phys. **88**, 213 (1988)
20. E.E. Ferguson, J. Am. Soc. Mass Spectrom. **3**, 479 (1992)
21. I. Korolov, R. Plasil, T. Kotrik, P. Dohnal, J. Glosik, Int. J. Mass Spectrom. **280**, 144 (2009)
22. L.D. Tsendin, Plasma Sources Sci. Technol. **12**, S51 (2003)
23. C.D. DeJoseph Jr., V.I. Demodov, A.A. Kudrjavtsev, Phys. Plasmas **14**, 057101 (2007)
24. K. Nanbu, Phys. Rev. E **55**, 4642 (1997)
25. R.R. Arslanbekov, A.A. Kudryavtsev, L.D. Tsendin, Phys. Rev. E **64**, 016401 (2001)
26. J. Glosik, I. Korolov, R. Plasil, O. Novotny, T. Kotrik, P. Hlavenka, J. Varju, I.A. Mikhaylov, V. Kokoouline, C.H. Greene, J. Phys. B: At. Mol. Opt. Phys. **41**, 191001 (2008)